Journal of Visualization, Vol. 4, No. 1 (2001) 81-90

Visualization of Flow Fields in a Bubble Eliminator

Tanaka, Y.*[1], Suzuki, R.*[2], Arai, K.*[1], Iwamoto, K.*[1] and Kawazura, K.*[1]

*1 Department of Mechanical Engineering, Hosei University, Kajinocho, Koganei-shi, Tokyo 184-8584, Japan.
*2 Opus System, Inc., 3-35-20 Okusawa, Setagaya-ku, Tokyo 158-0083, Japan.

Received 13 October 2000.
Revised 20 January 2001.

***Abstract*:** Bubbles and dissolved gases in liquids greatly influence the performance of fluid power systems, coating solutions, plants in the food industry and so on. To eliminate bubbles from working fluids and to prevent degradation of liquids as well as to avoid possible damage of fluid components is an important engineering issue. Recently one of the authors, Ryushi Suzuki, has developed a new device using swirling flow with the capability of eliminating bubbles and of decreasing dissolved gases in fluids. This device is called "Bubble Eliminator." The swirling flow pattern and pressure distributions in the bubble eliminator greatly influence the effective performance of the bubble removal. In this paper the swirl flow pattern in a transparent bubble eliminator is experimentally visualized and processed as digital images by a high-speed video camera system. Velocity profiles and pressure distributions in the bubble eliminator are calculated and graphically visualized by a three-dimensional numerical simulation. The results of the flow visualization are compared with the numerical simulation. The performance evaluation of the bubble removal effectiveness is numerically and experimentally verified. It is also proposed to augment understanding of 3D flow fields for the swirling flow in the bubble eliminator with scientific flow visualization methods, which combine graphics or real images with haptic displays.

***Keywords*:** bubble elimination, computational fluid dynamics, flow visualization, haptic interface, swirling flow.

1. Introduction

Bubbles and dissolved gases in liquids greatly influence the performance of fluid power systems (Backe and Lipphardt, 1976), coating solutions (Rauch and Sangl, 1999) and plants in the food industry. Especially bubbles in working fluids may cause major trouble of fluid power systems because of cavitation and aeration inception, bulk modulus change, degradation of lubrication (Yano and Yabumoto, 1991), noise generation, oil temperature rise and deterioration of oil quality (Matsuyama and Takesue, 1996). When the bubbles in oil are compressed adiabatically at high pressure condition, the temperature of the bubbles may rise sharply and the surrounding fluid temperature also rises. In a previous study (Suzuki et al., 1998), the authors have reported that the bubble elimination is useful for preventing oil temperature rise caused by bubbles in oil. Recent trends in industrial manufacturing are to compact machines and equipment in order to economize materials, energy consumption and required space. Therefore, it is important to eliminate bubbles from the liquid and to prevent degradation of the quality products and of the system performance as well as to avoid possible damage of the components.

One of the authors, Ryushi Suzuki has developed a new device using swirling flow with the capability of eliminating bubbles and of decreasing dissolved gases in liquids (Suzuki and Yokota, 1994). This device is called "Bubble Eliminator." The swirling flow pattern in a tapered tube chamber of the bubble eliminator greatly influences the effectiveness of bubble removal. Using the bubble eliminator enables the fluid power system to perform better through experiments (Suzuki et al., 1998).

With recent advances in computer performance, graphical techniques in visualizing simulation data are now achievable to display on computer workstations or personal computers. Most graphical techniques in scientific visualizations emphasize a global perspective to visualize scalar or complex 3D vector fields for simulation data. The graphical techniques are powerful tools to understand the simulation data in flow fields. Conventional graphical techniques, however, have not been able to provide locally realistic image and interactive sensation for representation of simulation data. Recently, the term "haptic interface" has begun to be used by human interface technologists to describe devices that stimulate the sensory capabilities within human hands. The word "haptic" means tactile and/or sense of touch. By using the haptic interface, one can sit down at a computer terminal and touch objects that exist only in the computer world. There have been a number of papers on the visualization of computational fluid dynamics data by means of the haptic interfaces (Avil and Sobierajski, 1996; Durbeck et al., 1998; Iwata and Noma, 1993).

In this paper three methods of scientific visualization techniques for the swirling flow of the bubble eliminator are adopted. Firstly the swirling flow pattern in a transparent bubble eliminator is experimentally visualized and processed as digital images by a high-speed video camera system. Images of time variant collected bubbles are presented by the flow visualization. Secondary the swirling flow patterns in the bubble eliminator are calculated by a three-dimensional numerical analysis for single-phase and multi-phase flow. The flow patterns are graphically visualized with a velocity vector field, a pressure contour and a profile of air particle content. The performance evaluation of the bubble eliminator is studied through visualization and numerical analysis of the swirling flow. Finally an interactive flow visualization system to understand flow fields through the simultaneous use of visual methods with the haptic interface is proposed and developed. The visual image data of real objects is mixed to the commercially available haptic interface; PHANToM (Massie, 1996) for the haptization data calculated from the position and the flow velocity.

2. Bubble Eliminator

The developed bubble eliminator is able to eliminate bubbles from liquids by means of a swirling flow. Figure 1 illustrates the principle of the bubble eliminator. The bubble eliminator consists of an inlet tube, a tapered tube and a straight tube. Liquids with bubbles flow tangentially into the tapered tube from an inlet port and form the swirling flow that circulates through the tapered tube. The swirling flow accelerates and the fluid pressure along the central axis decreases. From the end of tapered tube, the swirling flow decelerates and the pressure recovers toward the outlet. Since the mass density of the bubble is generally smaller than that of the liquid, air bubbles are trapped to the vicinity of the tube axis such as a centrifuge. The trapped bubbles are accumulated near the end of the tapered tube chamber where the pressure is the lowest. The trapped small bubbles merge and make a large air column in the vicinity of the tube axis. When a back pressure is applied at the downstream side of the bubble eliminator, the collected bubbles are ejected through a vent port. The actual figures and dimensions of the bubble

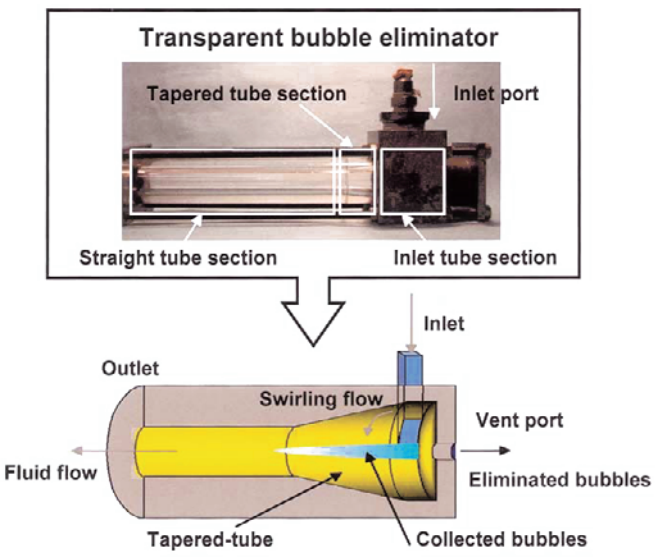

Fig. 1. Principle of bubble eliminator.

eliminator depend on the working fluid properties and the conditions of the flow rates. In a previous study (Suzuki and Yokota, 1994), it is experimentally confirmed that the bubble eliminator is able to eliminate bubbles and dissolved gases from the working fluid. The swirling flow pattern and the pressure distribution in the tapered tube chamber of the bubble eliminator greatly influence the effectiveness of the bubble removal in principle. The bubble eliminator has the advantage of a simple structure, a low level of the pressure drop (a few hundred Pa) and of being a passive element without any power supply.

3. Experimental Flow Visualization

Initially a full scale transparent model is used to the flow visualization in order to understand the situation of the collected bubbles. Figure 2 illustrates the experimental fluid circuit for the flow visualization. Working fluid in a 20*l* reservoir fed by a variable displacement-type piston pump flows to the transparent bubble eliminator. The tapered tube of the transparent bubble eliminator for the flow visualization is made from an acrylic pipe. An inlet tube section and a straight tube section have an inner diameter of 28 mm and 20 mm, respectively. A needle valve at the pump suction side is used experimentally to introduce air into the circuit. The needle valve is slightly opened and external air is admitted in the circuit for bubbling. For purposes of safety, a relief valve is set in the pump delivery line. The flow rate is measured by a flow meter in the downstream side of the fluid circuit. A solenoid-type on-off valve is installed on the vent port side of the bubble eliminator. The time interval of the vent valve closing is adjusted and monitored by a control circuit. In the usual case, the on-off valve is opened, and the trapped and collected bubbles are ejected through the vent line. When the on-off valve is closed, the trapped bubbles merge and make a large air column in a flash time. The high-speed camera (FASTCAM-ultima: maximum recording rate of 4300 frames per second) or the digital video camera is set at a flank of the transparent bubble eliminator. A growth pattern of the trapped bubbles by the swirling flow at the tapered tube in the bubble eliminator can be observed. The working fluid (Daphne Super Hydraulic Fluid #32) for oil hydraulic systems is used in the experiments of the flow visualization. The working fluid has a kinematic viscosity of 32 mm^2/s at the fluid temperature of 313K. The fluid flow rate is set at 20 *l*/min. For the flow rate of 20 *l*/min, the outlet side of the downstream tube has a fluid average velocity of 1 m/s and a Reynolds number of 700.

Figure 3 shows a snapshot of the digital video camera which shows a close-up photograph of the transparent bubble eliminator. The bubbles are collected along the central axis. A series of monochrome photograph frames obtained with the high-speed video camera is shown in Fig. 4. In the initial stage, when the elapsed time is zero, the on-off valve of the vent line is closed. When the on-off valve is closed, the trapped bubbles started to be collected and to form a large air column which extends along the central axis of the tube toward downstream. The photographs show that the air column grows into its maximum length within the first 0.1 second. The length of the air column increases from 17.5 mm to 47.5 mm through the series of frame digital images in accordance with the elapsed time. The growth process of the trapped bubbles with the elapsed time can be experimentally clarified through the flow visualization. A comparison between the experiments and the numerical results will be discussed in the next section.

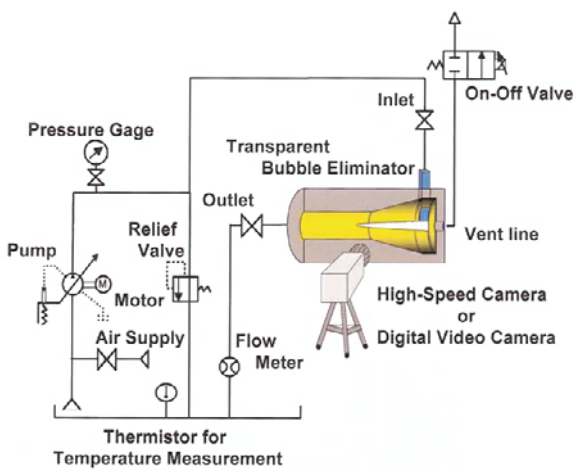

Fig. 2. Experimental fluid circuit for flow visualization.

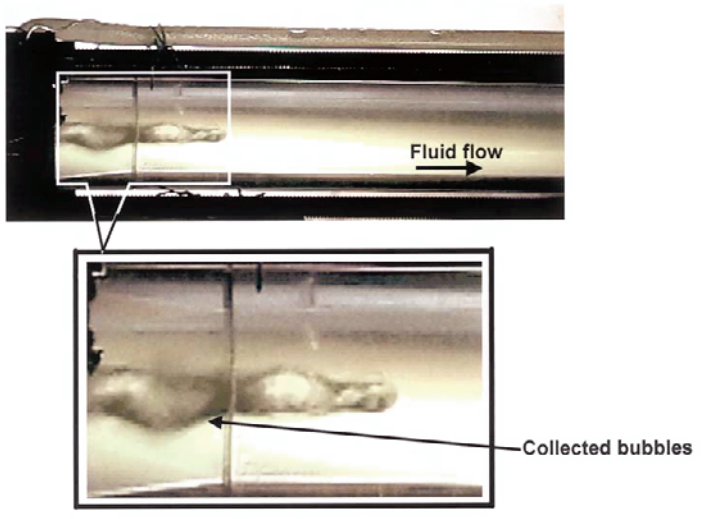

Fig. 3. Example photo of flow visualization with digital video camera.

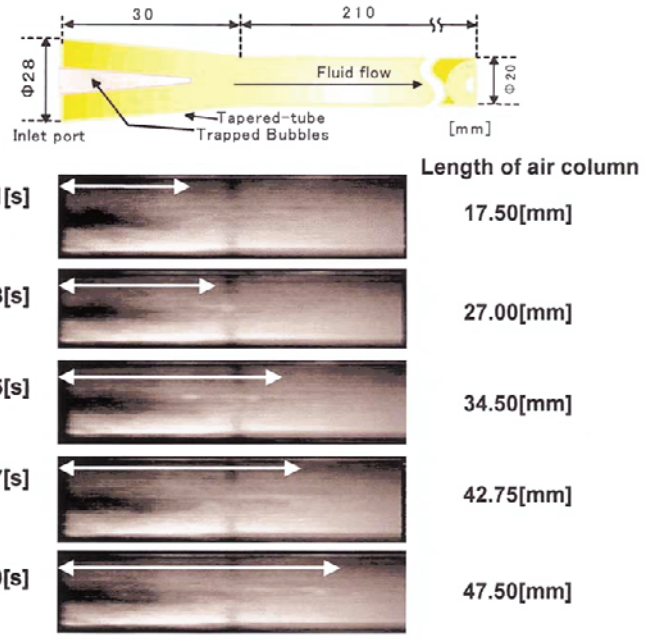

Fig. 4. Series photo of trapped bubbles with high-speed camera.

4. Numerical Simulation

Subsequently the swirling flow of the bubble eliminator by means of the numerical simulation is investigated. The steps of the numerical investigation consist of calculating for single-phase and multi-phase flow analyses, and displaying with graphics. The results obtained from the numerical calculation for the single-phase flow are made available as an initial condition of the numerical calculation for the multi-phase flow analysis. The swirling flow pattern, the velocity profile and the pressure distribution in the bubble eliminator are numerically calculated and graphically displayed by a three-dimensional numerical analysis.

Figure 5 shows the cells and the typical five definition blocks for the numerical analysis of the bubble eliminator. The overall apparatus for the bubble eliminator can be divided in the following blocks: an inlet port, a peripheral inlet tube, two tangential inlet ports, a tapered tube and a downstream tube. The two tangential inlet port regions are divided into smaller rectangles to account for fine velocity and pressure value fluctuation. There are 900 cells on the x-y plane of the tapered tube divided by use of the boundary-fit coordinate. The tapered tube and

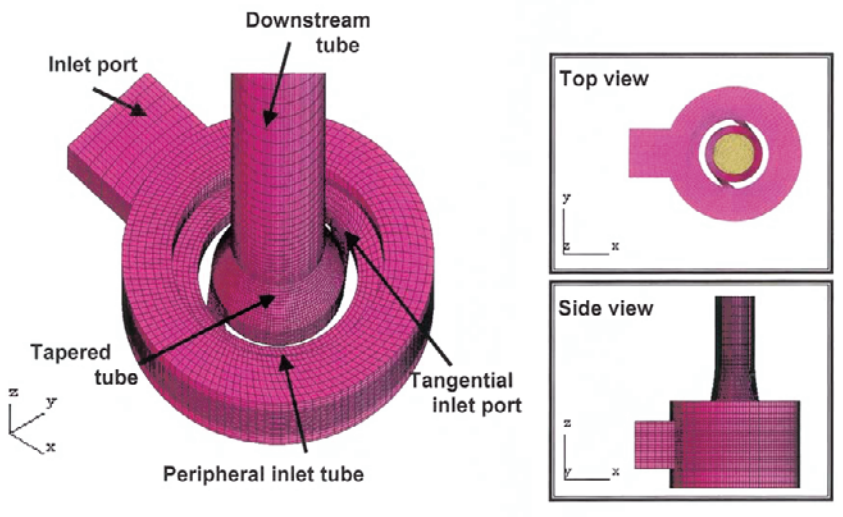

Fig. 5. Cells and definition of blocks for numerical analysis.

the downstream tube regions are non-uniformly divided into 55 cells along the z-axis. The number of total cells for the studied configuration including the peripheral inlet tube and the inlet ports is 81,000.

A three-dimensional flow analysis of an incompressible viscous flow by using the commercially available numerical calculation software, RFLOW (Rflow Co., Ltd.) is performed. Basic equations for the numerical analysis consist of the equation of continuity, the momentum equations and the energy equation. The basic equations are discretized by a finite volume method using boundary-fit coordinates and are solved by the successive over-relaxation (SOR) method. The numerical simulation has been performed for the working fluid having a kinematic viscosity of 30 mm^2/s, a density of 857 kg/m^3 and a flow rate of 20 *l*/min. The fluid properties in the numerical simulation are as same as those in the experimental flow visualization.

In the multi-phase flow analysis, it is assumed that the small air particles are mixed with the working fluid in the bubble eliminator. The diameter of the mixed particles kept at a constant value of 1 mm. Surface tension and buoyancy of the air particles are neglected. Time variant distribution of the collected air particles is calculated by the numerical results of the single-phase flow analysis for the initial values. The time interval of the numerical simulation for the multi-phase flow analysis is 0.1 ms.

A pressure distribution along the central axis C-D of the bubble eliminator is plotted at the top of Fig. 6. Pressure contours are also graphically shown in Fig. 6. All pressure data are related to the reference pressure at the end of the downstream tube. Initially, the pressure at the swirl center continuously decreases as the working fluid flows downstream. There is a minimum pressure point at the close end of the tapered tube which is indicated by a blue color oval region in the pressure contour. Subsequently, the pressure makes a gradual recovery along the center of the adjoining straight downstream tube, because the working fluid swirl falls in decay. Bubbles within the working fluid cannot escape to the downstream because of the positive pressure gradient. Finally, the pressure gradient returns negative because of the pressure drop.

A typical result of the calculated velocity profile and pressure distribution across the cross section of the inlet region is graphically illustrated in Fig. 7. The pressure distribution across the cross section (A-B) at the inlet region of tapered tube is also plotted in the same figure. The working fluid circulates through the peripheral inlet tube and is tangentially introduced into the tapered tube chamber from the two tangential inlet ports. Certain position-dependent centrifugal forces are presented in the swirl flow. If light particles are presented within the working fluid, these particles tend to move toward the central axis of the tube due to the difference in centrifugal force between the working fluid and the light particles. The pressure distribution drives bubbles to move toward the central axis. The forced swirl flow is symmetrically generated in the tapered-tube chamber. The flow pattern in each tangential inlet port is composed of the main stream from the peripheral inlet region and a small annular eddy enclosed between the main stream and the sharp-cornered wall of the tangential inlet port as shown in the magnified drawing of Fig. 7. The reverse flow caused by the small eddy in the tangential inlet port has an adverse effect on the performance of the forced swirl flow. Therefore, the swirl flow pattern and the magnitude of the inlet velocity have a great influence on the effectiveness of bubble removal by the bubble eliminator. The improvement

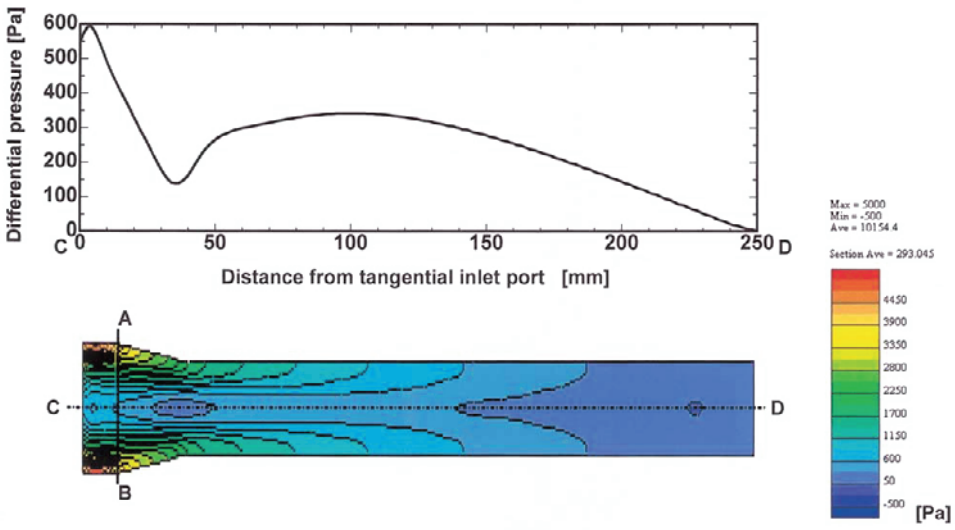

Fig. 6. Pressure distribution along central axis of bubble eliminator.

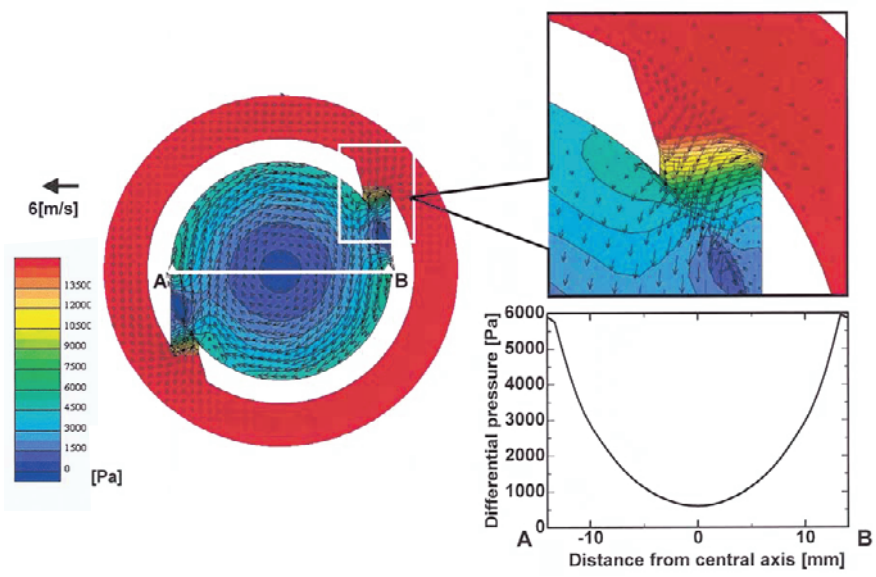

Fig. 7. Velocity profiles and pressure contour across inlet region.

of design parameters for the figures of the inlet port has been discussed in a previous paper (Tanaka et al., 1998; Tanaka et al., 2000).

A calculated content ratio of air particles along the central axis of the bubble eliminator is plotted in Fig. 8. The content ratio at the center of the swirl continuously increases as the working fluid flows downstream. There is a maximum value nearly the end section of the tapered tube. Figure 8 also graphically illustrates the typical numerical results of the percentage of the air content contour as a function of time for the multi-phase flow analysis. The distribution of the content ratio of the air particles is shown at every time interval of 0.01 second. At the initial stage when an elapsed time is zero, the fluid contains 3% air particles by volume all over the blocks. The air particles are collected near the end of the tapered tube and the columns tend to grow up near the central axis of the tube toward downstream.

In the numerical calculation for the multi-phase flow analysis, the bubbles are regarded as solid spheres without merging or collapsing. The volume of a sphere occupies 52% of total volume of a cube having each side as same as a diameter of the sphere. In other words the fluid numerically contains maximum 52% air particles by volume. In the numerical analysis, therefore, 52% of air content ratio becomes maximum efficiency of the trapped bubbles.

The growth rate of the air column is investigated as a function of the elapsed time from the results of the

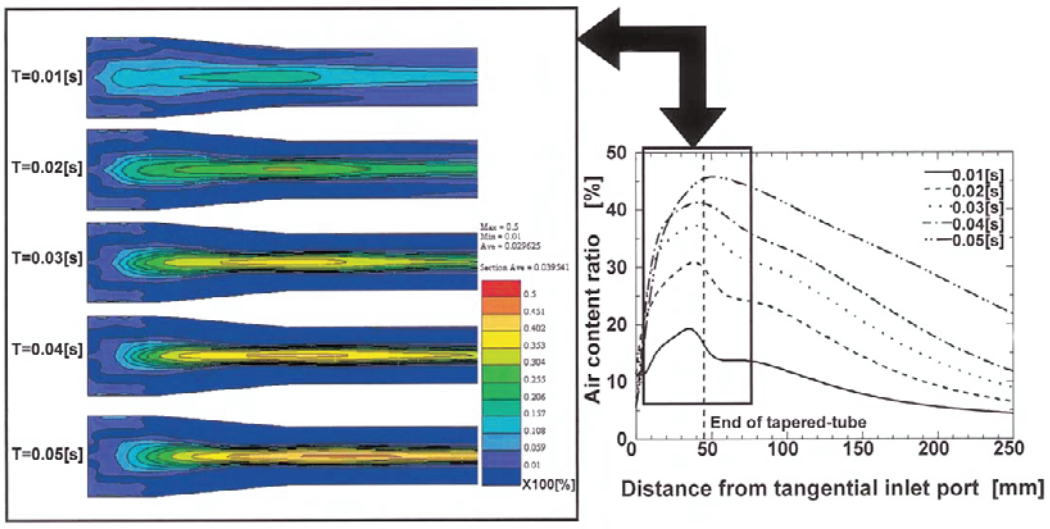

Fig. 8. Air particle content along central axis and contours as a function of time.

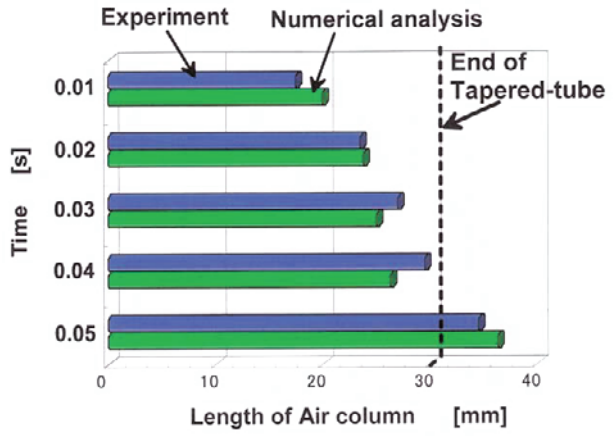

Fig. 9. Comparison between experiments and simulation for the length of air column.

numerical and the experimental flow visualization. Figure 9 shows the length of the air column with the elapsed by time comparing the results of numerical analysis with the experiments of the flow visualization. The actual length of the air column is obtained from the images of the experimental flow visualization reported in Fig. 3. In the case of the numerical analysis, the length of the air column is defined as the length between the inlet port and the point of the largest air content ratio of Fig. 8. The trapped bubbles are not carried on by the flow because the growth rate of the air column is smaller than the average flow velocity in the z-axial direction. The trapped bubbles behavior of the numerical analysis is qualitatively in good agreement with the experimental results of the flow visualization. Therefore, it is numerically and experimentally verified that the bubble eliminator collects bubbles effectively near the end of tapered tube.

5. Haptic Visualization

Finally in the scientific visualization techniques, it is proposed to augment the understanding of 3D flow fields for the swirling flow in the bubble eliminator with an interactive flow visualization method, which combines graphics or real images with haptic interfaces. The first computerized haptic interface was a force-reflecting teleoperation interfaced to computers that simulated the remote environment virtually (Batter and Brooks, 1972). Recently many practical and commercially available haptic interfaces have been developed and used in scientific visualizations or virtual reality works (Hollerbach, 2000). By using the haptic interfaces we can touch virtual objects that exist only

in computers. Tanaka and Aono (1998) developed a software model that enables force-reflecting haptic interaction to the uneven surface of materials represented with spatial distribution data.

In our proposed and developed system with haptics (Kawazura and Tanaka, 2000), the 3D flow field is arranged in a digital map with forces at the tip of the haptic interface. Figure 10 shows a configuration for displaying the visual and haptic sensations. The developed system consists of a personal computer for a haptic rendering, a SenseAble PHANToM (Personal HAptic iNTerface Mechanism developed by Massie, 1996) haptic device, a magic vision and an object with the flow field. The PHANToM has a desktop haptic probe that tracks the position of the operator's fingertip and exerts a precisely controlled external force on the fingertip in real time. To create convincing feel of touch the calculation loop for the haptic rendering occurs at a high renewal rate of 1 kHz.

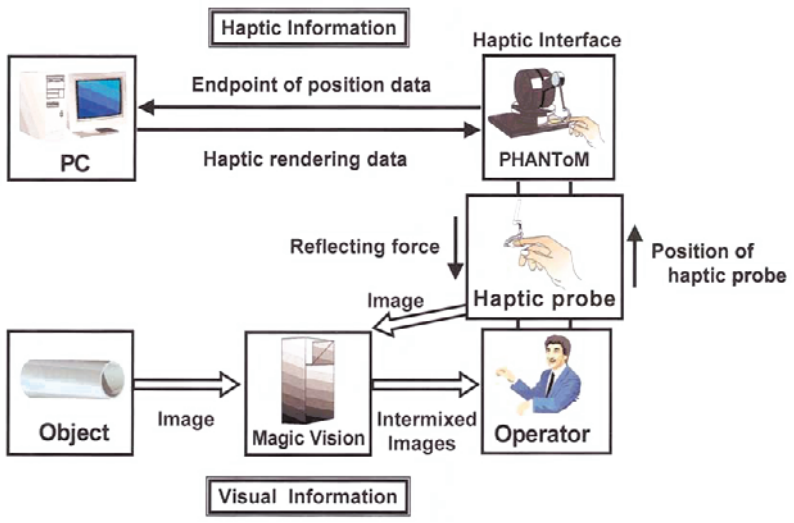

Fig. 10. System configuration for haptic visualization.

A 3D vector field is rendered and mapped into forces in the personal computer through the numerical simulation. The image of the real object such as a transparent pipe is intermixed with the operator's fingertip in the magic vision as shown in Fig. 11. The haptic probe of the PHANToM with the operator's fingertip penetrates virtually into the real object through hard surfaces of the object wall in the magic vision. The operator's fingertip with the haptic probe is controlled and forced by the endpoint of the PHANToM. One can virtually place his fingertip into the flow field and where the current is strongest and where the eddy exists. A photo of the object intermixed with the fingertip is shown in Fig. 12.

In comparison with the similarity between real and virtual touch in the flow field, the perceptual similarity is evaluated by a five-grade system to the sense of touch. Subjects were asked a question, "How would you rate the perceptual similarity of the haptic visualization?" The 37 answerers as the subjects have been accepted in my

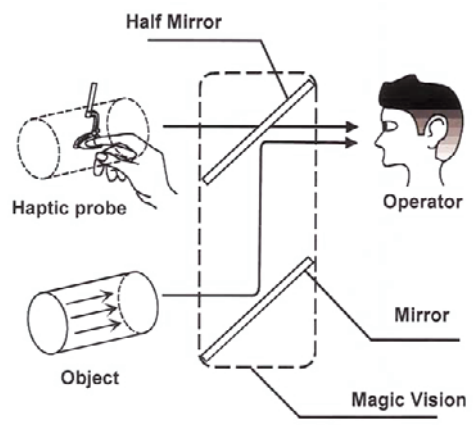

Fig. 11. Magic vision for intermixed images.

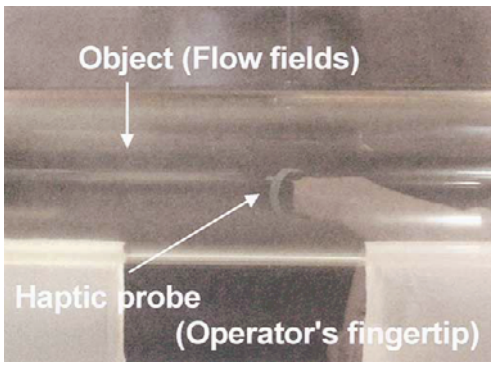

Fig. 12. Example photo of object intermixed with fingertip.

laboratory booth. The subjects, ranging in age from 20 to 68 years, made a choice of one answer that the rating grade scale is from "1 (lowest similarity)" to "5 (highest similarity)" after the several trials were provided. More than 80% subjects answered "I could feel the similarity (Grade 5)" or "I could mostly feel the similarity (Grade 4)" in the tests. Therefore, it is experimentally verified that one can feel and touch the virtual flow fields through the developed interactive flow visualization system.

6. Conclusions

In this paper the performance evaluation of the bubble eliminator is studied through the three scientific visualization techniques for the swirling flow. The scientific visualization techniques are effective tools to understand the behavior of the swirl flow in the bubble eliminator. As the results of the numerical analysis, the pressure distribution of the bubble eliminator for the swirl flow has a large influence on the performance of the bubble elimination. The results of the experimental flow visualization are qualitatively in good agreement with the results of the numerical analysis. To augment understanding of the 3D flow fields for the swirling flow in the bubble eliminator, it is also proposed and developed the haptic display system, which combines graphics or real images with the haptic display. By combining visual with the haptic interface, a better environment for the exploratory visualization of the swirling flow in the bubble eliminator is obtained. This overcomes the interactivity constraints of traditional flow visualization techniques. The haptic interaction provides new opportunities for insights to the comprehension of the scientific visualization. The results obtained from the new scientific visualization techniques bring forth much hope to establish design standards of the bubble eliminators in engineering fields. It can be considered that many problems caused by the entrained bubbles in fluid systems are solved by the bubble eliminator.

Acknowledgments

The numerical calculations have been performed at the Computational Science Research Center (CSRC) at Hosei University. The authors acknowledge with thanks the encouragement received from the staffs of the CSRC as well as the facilities of computations. The authors also wish to thank the staff at the Rflow Co., Ltd. for their technical suggestion on the numerical software. A part of this study has been carried out when one of the authors, Tanaka has stayed at the University of Utah as a visiting scholar. We are great thankful to Prof. John Hollerbach at the University of Utah for his valuable suggestions and support. Part of this paper has been presented in the sixth Triennial International Symposium on Fluid Control, Measurement and Visualization (FLUCOME 2000) in Sherbrooke, Quebec.

References

Avila, S. and Sobierajski, M., A Haptic Interaction Method for Volume Visualization, Proceedings of Visualization '96, (1996), 197-204.

Batter, J. and Brooks, F., Grope-1: A Computer Display to the Sense of Feel, Information Process, 71 (1972), 759.

Backe, W. and Lipphardt, Influence of the Dispersed Air on the Pressure, CI Mech. Eng., C97/76 (1976), 77-84.

Durbeck, L. J. K., Macias, N. J., Weinstein, D. M., Johnson, C. R. and Hollerbach, J. M., SCIRun Haptic Display for Scientific Visualization, Phantom Users Group Meeting (Dedham, MA), (1998-9).

Hollerbach, J. M., Some Current Issues in Haptics Research, Proc. IEEE Intl. Conf. Robotics and Automation (San Francisco), (2000-4), 757-762.

Iwata, H. and Noma, H., Volume Haptization, Proc. IEEE Symposium Research Frontiers in Virtual Reality (San Jose), (1993), 16-23.

Kawazura, K. and Tanaka, Y., Sensualization of Spatial Distribution Data in Flow Field, Research Bulletin of the Computational Science Research Center, Hosei University, Vol.13 (2000), 7-13 (in Japanese).

Massie, T., Initial Haptic Explorations with the Pahntom: Virtual Touch through Point Interaction, Master Thesis at MIT, (1996-2).
Matusyama, Y. and Takesue, M., Introduction of Non-sludge Type Hydraulic Fluids, Proceedings of 3rd JHPS International Symposium on Fluid Power (Yokohama), (1996), 613-616.
Rauch, R. and Sangl, R., Gasses in Coating Colors -Their Impact on Runnability and Their Measurement, TAPPI Coating Conference Proceedings, (1999), 357-370.
Suzuki, R. and Yokota, S., Bubble Elimination by Use of Swirl flow, IFAC Int. Workshop on Trends in Hydraulic and Pneumatic Components and Systems (San Francisco), Poster Paper 2, (1994).
Suzuki, R., Tanaka, Y. and Yokota, S., Reduction of Oil Temperature Rise by Use of a Bubble Elimination Device in Hydraulic Systems, Journal of the Society of Tribologists and Lubrication Engineers, 54-3 (1998), 23-27.
Suzuki, R., Tanaka, Y., Arai, K. and Yokota, S., Bubble Elimination in Oil for Fluid Power Systems, SAE Transactions, Journal of Commercial Vehicles, Section 2, Vol.107 (1998), 381-386.
Tanaka, Y., Suzuki, R., Yamamoto, H., Arai, K., Iwasaki, H. and Oguchi,Y., Numerical Analysis of Swirl Flow in Bubble Elimination Device, Proc. ASME Fluid Engineering Division Summer Meeting (FEDSM'98), (Washington D.C.), (1998-6).
Tanaka, Y. and Aono, T., Haptic Interface for Enhanced Sensation of Spatial Distribution Data, Proceedings Vol.1 of 5th International Conference on Control, Automation, Robotics and Vision (ICARCV '98) (Singapore), (1998), 415-418.
Tanaka, Y., Suzuki, R., Arai, K. and Iwamoto, K., Numerical Simulation and Visualization of Swirling Flow in Bubble Eliminator, Proceedings of 48th National Conference on Fluid Power (Chicago), (2000-4), 251-261.
Yano, H. and Yabumoto, J., Expected Development of the Bubble Elimination Device for Fluids, Mitsubishi Oil Co. Technical Review, No.76 (1991), 117-126.

Authors Profile

Yutaka Tanaka: He earned a degree of Dr. Engineering from Tokyo Institute of Technology, Japan in 1991. From 1985 to 1991, he worked in the Precision and Intelligence Laboratory, Tokyo Institute of Technology as a Research Associate. Since 1991, he has been Associate Professor of Mechanical Engineering at the College of Engineering, Hosei University, Tokyo, Japan. From 1999 to 2000, he stayed at the School of Computing, the University of Utah as the Visiting Associate Professor. He is a member of the Japan Hydraulics & Pneumatics Society (JHPS), Japan Society of Mechanical Engineers (JSME), the Society of Instrument and Control Engineers (SICE), Robotics Society of Japan, Institute of Electrical Engineers of Japan (IEE) and Virtual Reality Society of Japan (VRSJ).

Ryushi Suzuki: He received a B.S. degree in Mechanical Engineering from Yokohama National University in 1953. From 1953 to 1989, he worked at Ishikawajima Heavy Industries Co. and its subsidiary as a designing engineer developing hydraulic systems for rolling mill, press and other machinery. From 1990 to 1997, he was the president of OPUS Corporation and currently is the president of Opus System, Inc. He is a council member of the Japan Hydraulics and Pneumatics Society (JHPS) and a member of the Japan Society of Tribologists and the Society of Tribology and Lubrication Engineers (STLE). He received the JHPS R&D Award for the bubble elimination device in 1995 and the JHPS Award for technical contribution in 1997.

Kazuyoshi Arai: He earned a degree of Dr. Engineering from Tokyo Institute of Technology, Japan in 1988. From 1988 to 1993, he worked as a Research Associate at the Faculty of Engineering, Yokohama National University. From 1993 to 1995, he worked at the College of Industrial Engineering, Nihon University as a Research Associate. Since 1995, he has been Associate Professor of Mechanical Engineering at the College of Engineering, Hosei University, Tokyo, Japan. He is a member of Japan Society of Mechanical Engineers (JSME), the Society of Chemical Engineers, Japan (SCEJ), and the Society of Materials Science, Japan (JSMS).

Kazuhiko Iwamoto: He received a B.S. degree in Mechanical Engineering from Hosei University in 1999. He is a master course student at the Graduate School of Mechanical Engineering, Hosei University.

Kenji Kawazura: He received B.S. and M.S. degrees in Mechanical Engineering from Hosei University in 1998 and 2000. Since 2000, he works in Asahi Optical Co., Ltd.